Characterizing ultrashort pulses with photon energies above 1.12 eV based on transient absorption in silicon thin films
Supplementary Data

Mayank Kumar[1], Saadat Mokhtari[1,2], Tristan Guay[1], Adrien Leblanc[3], Kosta Oubrerie[4], Sohail A Jalil[2], Elissa Haddad[1], Gaëtan Jargot[1], Philippe Lassonde[1], Heide Ibrahim[1,5], Giulio Vampa[2], and François Légaré[1]

[1]Advanced Laser Light Source (ALLS), Centre Énergie Matériaux Télécommunications, Institut National de la Recherche Scientifique (INRS-EMT), 1650 Boulevard Lionel-Boulet, Varennes, Québec J3X 1P7, Canada
[2]Joint Attosecond Science Laboratory, National Research Council of Canada and University of Ottawa, 100 Sussex Drive, Ottawa, Ontario K1A 0R6, Canada
[3]Laboratoire d'Optique Appliquée, Ecole Polytechnique, ENSTA, CNRS, Université Paris Saclay, Palaiseau, France
[4] Université Paris-Saclay, CEA, LIDYL, 91191 Gif-sur-Yvette, France
[5] Department of Physics, University of Ottawa, 150 Louis-Pasteur Pvt, Ottawa, Ontario K1N 6N5, Canada

S1 Experimental Setup

The experimental setups for generating probe pulses (sub-20 fs visible pulses and the supercontinuum) are shown in Figure S1. FROSt is a pump-probe method-based pulse characterization technique, which inherently demands a pump beam synchronized with the pulses to be characterized (or probe). Thus, the fundamental output of the laser (1030 nm) was divided into two parts using a variable attenuator (VA) to generate pump and probe pulses.

First, to generate sub-20 fs visible pulses (Figure S1 (a)), the fundamental output at 1030 nm ($\sim$ 135 μJ per pulse) was spectrally broadened in a 0.9-m-long methane-filled hollow core fiber (HCF, *few-cycle* Inc.) with an inner diameter of 250 μm [1, 2]. The HCF was maintained at a static gas pressure of 4.5 bar. The power-dependent nonlinear dispersion (or SPM) in CH_4 leads to the spectral broadening of the fundamental pulses [2]. The positive chirp acquired by the fundamental pulses at the HCF output was compensated using highly dispersive mirrors (PC1611, UltraFast Innovations GmbH) to achieve a pulse duration of $\sim$ 29.5 fs. The retrieved results from the SHG-FROG characterization of the compressed fundamental pulses are shown in Figure S2. A part of the compressed output ($\sim$ 3.75 μJ per pulse) was frequency doubled in a 25 μm-thick β-Barium Borate (BBO) crystal to obtain sub-20 fs broadband visible pulses centered at 515 nm. These pulses were focused onto the SOS sample using a gold off-axis parabolic mirror (OAP-1), as shown in Figure S1 (a). The energy of the probe pulse measured at the position of the SOS was 220 nJ.

To determine the repetition rate scalability of the FROSt method using thin Si films, we used argon (Ar) gas instead of CH_4 for spectral broadening of the fundamental output of the laser. The reason for choosing an atomic gas is that molecular gases exhibit thermal effects at high average power and higher repetition rates, affecting the transmission through the HCF and spectral broadening at the output [3]. The setup to generate broadband visible pulses remained the same, as shown in Figure S1 (a). A pressure gradient was created along the length of the HCF by maintaining an Ar pressure of 3.5 bar at the HCF output and pumping out the gas at its input. The HCF input was kept at a low pressure ($<$ 10 mbar) to avoid any thermal effects that could affect the coupling into the fiber. The spectrum of the fundamental pulses at the HCF output is shown in Figure S3.

To generate SC probe pulses, the gas-filled HCF was replaced by a 4 mm-thick YAG window. The SC was generated using 1030 nm pulses with 23.5 μJ energy. The central part of the beam coming out of the window was spatially selected using an iris. The spectral components of the SC probe were filtered using a shortpass filter (FES0850, Thorlabs, Inc.), as shown in Figure S1 (b). The probe energy after the filter was below the detection limit of our energy meter (< 200 nJ). Based on the integration time required to observe the same photon count as that in the case of the ultrashort pulses, the energy of the probe pulse can be estimated to be less than 100 nJ per pulse.

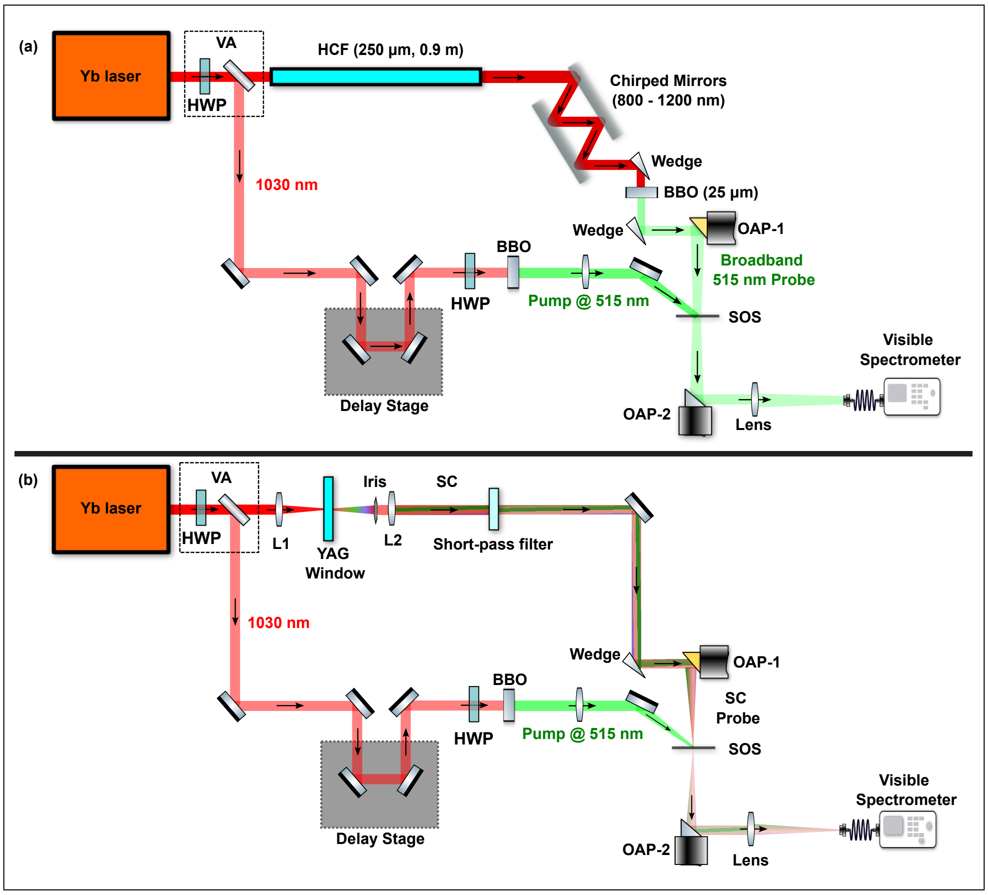

Figure S1: Schematic of the experimental setup: The fundamental output of the Yb laser (Tangerine, λ_F = 1030 nm was divided into two parts using a variable attenuator (VA). One part of the output, passing through the delay stage and a half-waveplate (HWP @ 1030 nm), was used to generate a pump (λ_P = 515 nm) by employing SHG in 1.5 mm thick BBO. For probe generation, we used two methods: (a) by frequency-doubling the temporally compressed broadband output λ_F = 1030 nm) generated using a gas-filled HCF (*few-cycle*, Inc.) and highly dispersive mirrors (PC1611, Ultrafast Innovations GmbH); (b) by spectrally selecting the visible part of SC generated in 4 mm thick YAG window. The probe beam was attenuated using wedge(s) in both methods. It was then focused on the SOS sample (500 nm thick Si-film on 460 μm thick sapphire substrate, MTI Corporation) using a gold-polished off-axis parabolic mirror (OAP-1) to achieve $\leq$ 200 nJ per pulse energy of probe pulses. The transmitted probe beam was collimated using a silver-polished OAP (OAP-2) and then focused into a Si-detector-based visible spectrometer (Avantes - AvaSpec-ULS2048CL-EVO). The pump delay stage is scanned, and the transmitted spectrum of the probe pulses with respect to the delay between pump λ_P = 515 nm and the probe is recorded to obtain FROSt spectrograms.

S2 FROG trace

The ultrashort visible pulses described in Section S1 were generated by frequency-doubling the compressed fundamental output of the Yb laser (Tangerine, Amplitude Laser Systems). The compressed output was characterized using FROG; the results are shown in Figure S2.

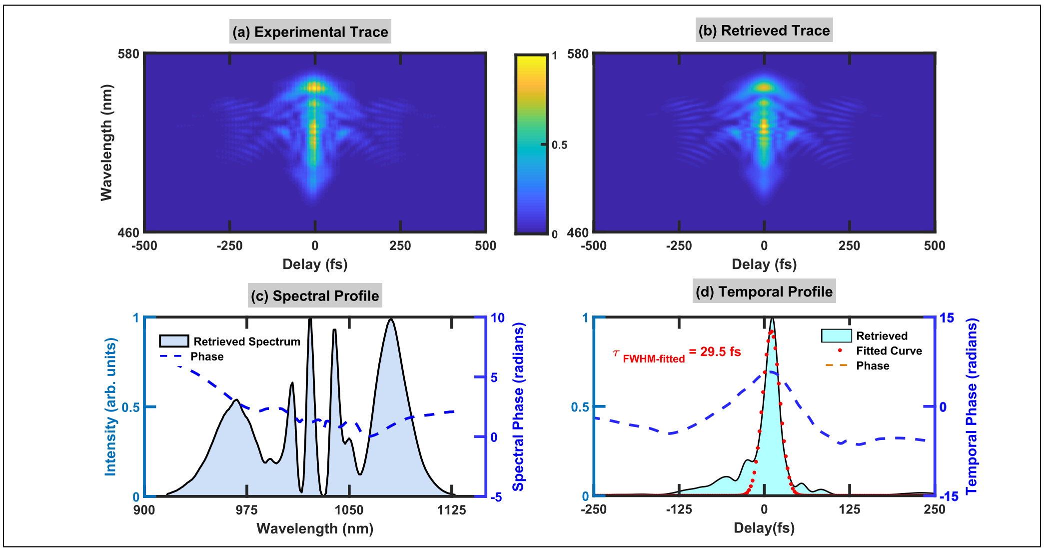

Figure S2: Characterization of CH_4-filled HCF output:(a) Experimental FROG trace; (b) reconstructed FROG trace; (c) retrieved spectral intensity (shaded blue, black outline) and spectral phase (dashed blue line); (d) retrieved temporal intensity (shaded light blue, black outline) and temporal phase (dashed blue line). A Gaussian curve was fitted to the temporal intensity curve to determine the full-width at half-maximum (FWHM) temporal duration of the output (red dots), $\tau_{\mathrm{FWHM}} = 29.5$ fs.

S3 Spectral Broadening in Argon

The fundamental output of the laser was spectrally broadened using Ar-filled HCF, and acquired dispersion was compensated using highly dispersive mirrors for repetition rate scalability experiments. Figure S3 shows the spectrum of the HCF output when the laser was tuned to a repetition rate of 250 kHz. Visible pulses generated by these pulses were characterized using silicon-on-sapphire (SOS) samples, and the results are shown in **Figure 4** of the main manuscript.

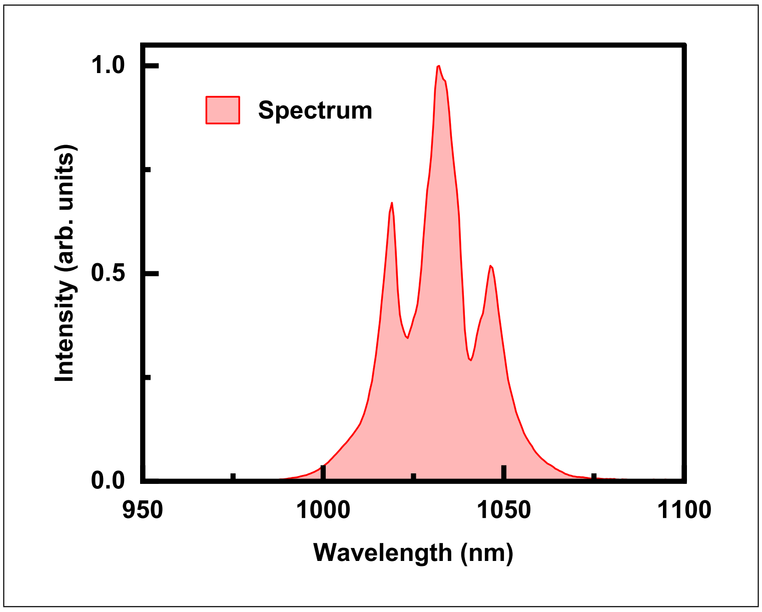

Figure S3: Spectral broadening in Ar-filled HCF : The spectrum of the fundamental ($\lambda_F = 1030$ nm) pulses at the HCF output at a repetition rate of 250 kHz is shown in shaded red. At the HCF input, the power was 38.46 W. Total output power was 28.30 W.

S4 Calculation of spectral phase using Sellmeier Equations

The Sellmeier equations used to compute refractive indices of Zinc Sulphide (ZnS) [4] and Barium Fluoride (BaF_2) [5] in between 460 - 900 nm are given below:

(i)

$$n_{ZnS}^2 = 8.393 + \frac{0.14383}{\lambda^2 - 0.2421^2} + \frac{4430.99}{\lambda^2 - 36.71^2} \tag{A1}$$

(ii)

$$n_{BaF_2}^2 = 1.33973 + \frac{0.81070\lambda^2}{\lambda^2 - 0.10065^2} + \frac{0.19652\lambda^2}{\lambda^2 - 29.87^2} + \frac{4.52469\lambda^2}{\lambda^2 - 53.82^2} \tag{A2}$$

For a given material of length L, the spectral phase change ($\varphi(\omega)$) induced by the material can be calculated by:

$$\varphi = \frac{L\omega}{c}.n(\omega) \tag{A3}$$

In the FROSt reconstruction results, we obtain the probe's electric field as a function of angular frequency ($\tilde{E}(\omega)$), which can be used to calculate the spectral phase ($\varphi_{ret}(\omega)$).

$$\varphi_{ret}(\omega) = \arg(\tilde{E}(\omega)) \tag{A4}$$

Using Taylor expansion, the spectral phase $\varphi_{cal}(\omega)$ can be expressed as (up to first order term around the central frequency ω_0:

$$\varphi(\omega) \approx \varphi(\omega_0) + (\omega - \omega_0)\left(\frac{d\varphi}{d\omega}\right)_{\omega_0} \tag{A5}$$

Using the equation A3, the $\varphi(\omega)$ can be expressed in terms of refractive index as follows:

$$\varphi(\omega) \approx \varphi(\omega_0) + (\omega - \omega_0)\frac{L}{c}\left(n(\omega_0) + \omega_0\left(\frac{dn}{d\omega}\right)_{\omega_0}\right) \tag{A6}$$

Further, using the refractive index calculated with the Sellmeier equations (equations A1 and A2) and centering the minima of the spectral phase to the central wavelength (λ_0), the spectral phase can calculated as:

$$\varphi_{cal}(\omega) = n(\lambda)\frac{L\omega}{c} - (\omega - \omega_0)\frac{L}{c}\left(n(\lambda_0) - \lambda_0\left(\frac{dn}{d\lambda}\right)_{\lambda_0}\right) - n(\lambda_0)\frac{L\omega_0}{c} \tag{A7}$$

S5 Supercontinuum Generation in YAG

The experimental setup used to generate supercontinuum (SC) in visible is described in **Section S1**. The spectrum of the SC generated using a 4 mm thick YAG window was recorded using a Si-detector-based visible spectrometer (Avantes - AvaSpec-ULS2048CL-EVO) and is shown in Figure S4 (shaded red, red outline). The visible part of the supercontinuum was spectrally filtered for characterization using a short-pass filter FES0850 (Thorlabs, Inc.) and is shown in Figure S4 (gradient fill, black outline). The modulations in the filtered spectrum towards the shorter wavelengths (560-600 nm) are due to the amplitude modulation caused by the short-pass filter [6].

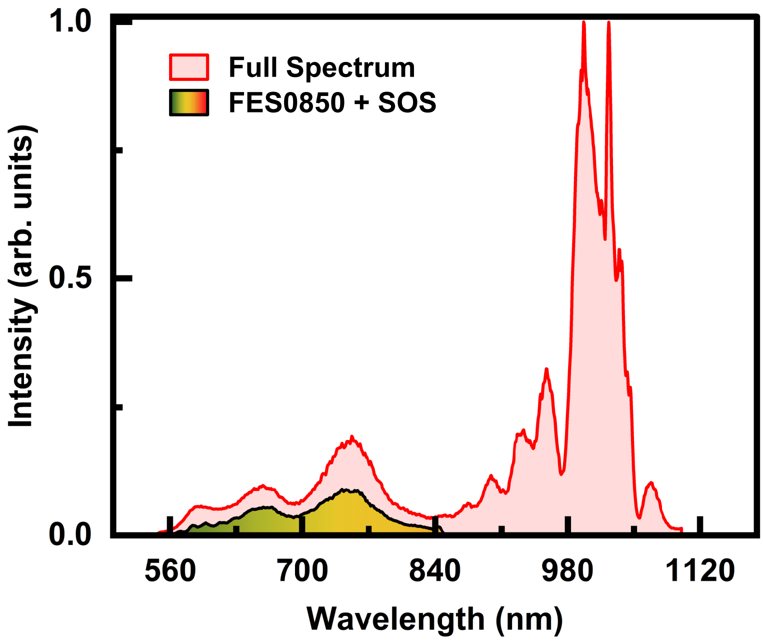

Figure S4: Supercontinuum generation in YAG window : (a) SC was generated using a 4 mm thick YAG window and recorded using a Si-detector-based visible spectrometer, which is shown in shaded red. The NIR part of SC is not included here; (b) the spectrum of the spectrally filtered part (after short-pass filter FES0850) is shown with a black outline and gradient fill.

S6 Transmittance through the Silicon thin films

In an absorbing medium with absorption coefficient α, the transmitted intensity of the incident beam with an intensity I_0 decreases exponentially as the light propagates through the medium. The transmitted intensity after length L is given by:

$$I(L) = I_0.exp(-\alpha.L) \tag{A8}$$

Similarly, Si is also an absorbing medium, which results in wavelength-dependent absorption of light in it. The typical transmittance of light through the Si thin films of 500 nm thickness is shown below [7, 8]:

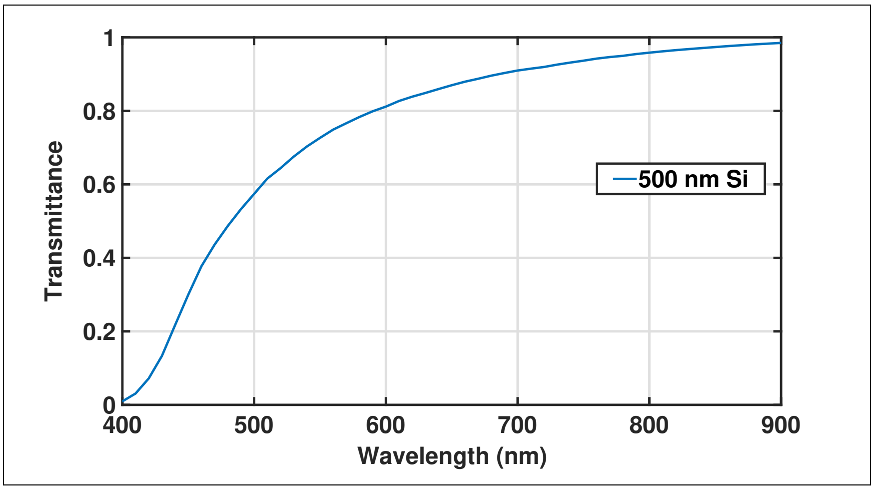

Figure S5: Transmittance of 500 nm thick Si films: The transmittance of Si thin films depends on the wavelength-dependent absorption coefficient α. As α increases for shorter wavelengths, transmittance decreases towards 400 nm, which can be inferred from equation A8.

In our case, the sample SOS does not affect the spectral bandwidth of the ultrashort pulses, resulting in high-confidence retrieval of their temporal characteristics, as seen in the Figure S6 below:

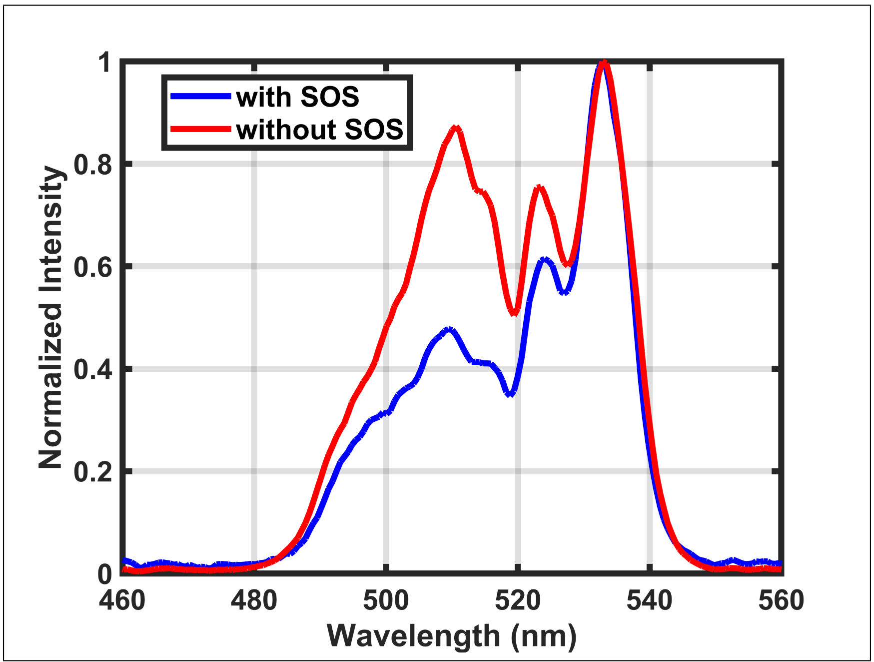

Figure S6: Linear absorption in SOS: The spectral profile of ultrashort probe pulses before (red solid line) and after (blue solid line) SOS. The difference in intensity in the latter case is due to the linear absorption in Si thin film.

References

[1] Nisoli M, De Silvestri S, Svelto O, Szipöcs R, Ferencz K, Spielmann C, et al. Compression of high-energy laser pulses below 5 fs. Opt Lett. 1997 Apr;22(8):522-4.

[2] Kwon O, Safaei R, Lassonde P, Fan G, Baltuška A, Schmidt BE, et al. Raman effect in the spectral broadening of ultrashort laser pulses in saturated versus unsaturated hydrocarbon molecules. Opt Express. 2020 Jan;28(2):980-90.

[3] Beetar JE, Nrisimhamurty M, Truong TC, Liu Y, Chini M. Thermal effects in molecular gas-filled hollow-core fibers. Opt Lett. 2021 May;46(10):2437-40.

[4] Debenham M. Refractive indices of zinc sulfide in the 0.405–13-μm wavelength range. Appl Opt. 1984 Jul;23(14):2238.

[5] Li HH. Refractive index of alkaline earth halides and its wavelength and temperature derivatives. J Phys Chem Ref Data. 1980 Jan;9(1):161-290.

[6] Thorlabs.com-FES0850-Catalog-Obsolete-Product; 2023. Webpage: https://www.thorlabs.com/catalogpages/obsolete/2023/FES0850.pdf.

[7] Green MA. Self-consistent optical parameters of intrinsic silicon at 300K including temperature coefficients. Sol Energy Mater Sol Cells. 2008 Nov;92(11):1305-10.

[8] Polyanskiy MN. Refractiveindex.info database of optical constants. Sci Data. 2024;11(1).